The 56th International October Conference on Mining and Metallurgy
22-25 October 2025, Bor Lake, Bor, Serbia
www.ioc.tfbor.bg.ac.rs

DOI: 10.5937/IOC25269I
Original scientific paper

THERMODYNAMIC INVESTIGATION OF CARBOTHERMIC REDUCTION OF ELECTRIC ARC FURNACE DUST

Angel Iliev[1a], Daniela Grigorova[1b]

[1] University of Chemical Technology and Metallurgy, 8 Kl. Ohridsky blvd., 1756 Sofia, Bulgaria
[1a] angel.iliev@kcm.bg, 0009-0002-1768-1300
[1b] d.dimitrova@uctm.edu, 0000-0001-8440-4368

Abstract
Electric arc furnace dust (EAFD) is a by-product generated after the gas cleaning systems in the steelmaking industry. This material is among the fastest-growing types of industrial waste and is classified as hazardous due to its high content of metal oxides. The management and utilization of EAFD represent a key aspect of sustainable industrial practices and circular economy principles. In the present study, waste dust samples from three different steel production sources were characterized. The chemical composition and properties of the dusts were determined. The thermodynamics of reduction processes for both synthetic and real mixtures were investigated using a galvanic cell method. The equilibrium oxygen pressure was determined by EMF measurements. The emphasis is on the thermodynamic features of zinc extraction. Based on experimental data, the dependencies of ΔG = f(T) were derived. The initial reduction temperature and the optimal amount of carbon were determined.

Keywords: *electric arc furnace dust (EAFD), steel, zinc, thermodynamics, EMF measurement*

1. INTRODUCTION

The electric arc furnace (EAF) production is one of the most well-known processes for steel production [1-3], due to its flexibility in operations, lower capital investments, and the ability to use up to 100% scrap. About 20 kg of dust is generated for every ton of steel produced [4-6]. The waste dust has different sizes and shapes [7], depending on the process, the type and composition of the scrap used, and the type of steel grade. The formation of the dust is complex and involves the evaporation and subsequent condensation of volatile elements and process-generated particles [1, 6, 8]. The resulting dust in the gas phase is captured by gas cleaning equipment, mainly by bag filters or electrostatic precipitators. The captured dust from the electric arc furnace (EAF) contains on average about 19 mass % zinc and 3 mass % lead [1, 4, 6]. Worldwide, the dust from electric arc furnaces is not fully utilized. Due to its high zinc content, the main focus is on its extraction. Several studies have been conducted using pyrometallurgical [6, 7, 9] and hydrometallurgical routes [5] for the recovery of zinc from electric arc furnace dust (EAFD). Most pyrometallurgical methods, such as the Waelz process, sintering, FASTMET and FASTMELT, OXYCUP, ZincOX, Primus, and ArcFume, are based on high-temperature reduction of EAFD using a suitable reducing agent such as carbon, carbon monoxide, or hydrogen gas [10, 11]. Carbothermal reduction uses carbon, most often in the form of coke breeze, as the reducing agent. The process occurs at temperatures above 1000°C, with a high consumption of fluxes and coke. Processes using coke (coke breeze) are energy-intensive pyrometallurgical technologies and lead to significant emissions of greenhouse gases, especially CO_2 [13]. The purpose of this investigation is to optimize the processes for recovering the zinc contained in electric arc furnace dust, based on a thermodynamic assessment of its reduction.

2. EXPERIMENTAL

In this work, waste dusts from electric steelmaking processes at iron and steel plants in the Republic of Bulgaria (BG), the Republic of Greece (GR), and the Republic of Serbia (RS) were

investigated. The chemical composition is determined by ICP analysis and is represented in Table 1. The sieve analysis was carried out according to ISO 13796:2012 standard. The sieving was carried out on a shaking machine. The structure and phase composition were determined by X-ray diffractometer (PANalytical Empyrean) and computed X-ray microtomograph.

The thermodynamic properties of phase reactions in ZnO-Zn, Fe_2O_3-ZnO-C, and the multicomponent real system of EAFD have been studied by electromotive force (EMF) measurements in a concentration galvanic cell - a galvanic cell with a solid electrolyte ZrO_2 and a reference electrode Ni/NiO:

$$\underset{P'_{O_2}}{\text{Pt}|\ \textit{studied mixture}\ |}\ |\text{ZrO}_2(\text{CaO})\ |\ |\ \underset{P''_{O_2}}{\textit{NiO, Ni}|\ \text{Pt}} \qquad (1)$$

3. RESULTS AND DISCUSSION

According to the chemical composition (Table 1), the iron content is in the range from 22.97% to 24.05%, and zinc is in the range of 25.66%-29.79%. The X-ray diffraction patterns of the three materials are presented in Figures 1 to 3. The main predominant phase in the three samples is magnetite (Fe_3O_4) with a spinel-type structure and zinc oxide. In sample 1BG, the main phases are zinc oxide (ZnO) - 30.8%, Magnetite (Fe3O4) 53.2%, Diopside (CaMgO6Si2)- 15.1%, and Litharge (PbO) – 0.7%. The main phase in sample 2GR is Fe_3O_4 - 43.2%, and zinc oxide is 17.5%. In this powder, a higher content of $CaMgO_6Si_2$ - 38.9% was determined. This indicates that this dust was generated from a process using steel scrap having less galvanized materials in a higher oxidizing environment. Sample 3RS contains the highest percentage of zinc oxide – 39.9% and 51.8% Magnetite. The Diopside content is the lowest compared to the other two samples, 7.6%. The result of the performed magnetic separation shows a magnetic fraction of over 96-99%.

Table 1. Main chemical compositions of EAFD (wt.%)

Source	Moisture	Zn	Fe	Pb	Cu	Al	SiO_2	CaO	MgO
1BG	6.56	24.75	38.48	2.06	0.27	0.64	3.71	6.52	3.42
2GR	11.37	17.60	31.25	3.36	0.23	0.55	4.06	5.55	1.76
3RS	16.70	31.79	37.50	2.14	0.23	0.60	3.60	4.38	0.94

Table 2 presents the theoretically derived thermodynamic equations for the change in Gibbs free energy as a function of temperature. The samples were dried and quartered. Depending on their availability and considering their mutual recycling, a mixture was made with a percentage ratio of 1BG:2GR:3RS - 30:40:30.

Table 2. Thermodynamic parameters (A and B) for $\Delta G^0 = A + B \cdot T$

Reaction	**A (J/mol)**	**B (J/mol·K)**	**No.**
ZnO (s) + C (s) → Zn (g) + CO (g)	247891	−209.18	(2)
ZnO (s) + C (s) → Zn (g) + CO_2 (g)	314114	−225.83	(3)
ZnO (s) + CO (g) → Zn (g) + CO_2 (g)	66223	−16.654	(4)
ZnO (s) + Fe (s) → Zn (g) + FeO (s)	87017	+210.02	(5)
ZnO (s) + C (s) + CO (g) → Zn (g) + CO_2 (g)	380501	−242.65	(6)
Fe_3O_4 (s) + CO (g) → 3FeO + CO_2 (g)	35386	−40.166	(7)
Fe_3O_4 (s) + C (s) → 3FeO (s) + CO (g)	236403	−231.9	(8)

A sieve analysis was carried out. The distribution by fractions is presented in Figure 4. The density of the powders was determined pycnometrically using a wetting component of ethyl alcohol. The determined density was 0.4136 g/cm^3. The fractional distribution after sieve analysis showed that the largest portion of the material (31.16%) falls within the 0.20–0.32 mm size range, indicating a predominantly fine-grained composition.

Zinc oxide does not decompose on heating at ordinary temperatures, but remains stable up to very high temperatures (~1975°C). Figure 5 shows the dependence of mass loss in percent on temperature during carbothermic reduction. It can be seen that by increasing temperature, the reduction becomes more intense, and at 1400°C, the mass loss reaches about 85%. The dependence of the percentage recovery of zinc on the carbon content in the carbothermic reduction of zinc oxide is presented in Figure 6.

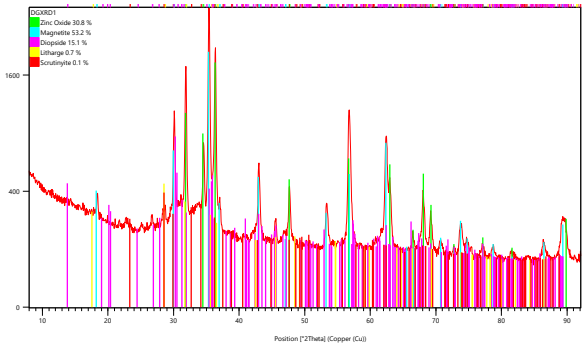

Figure 7. XRD pattern of 1BG EAFD sample

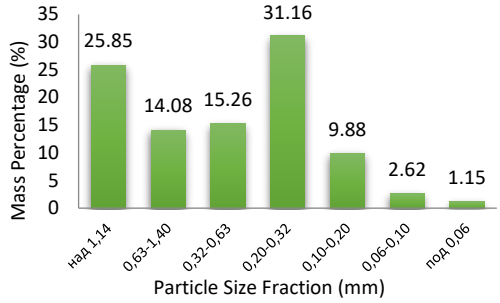

Figure 4. Particle size distribution of EAFD

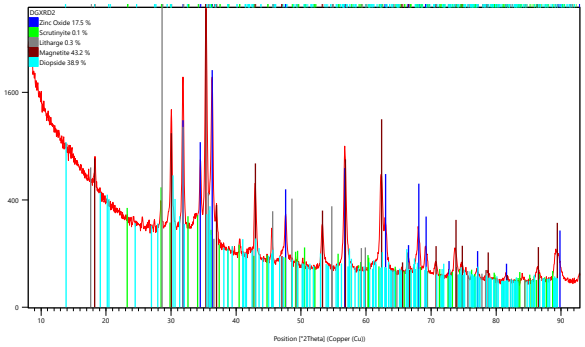

Figure 8. XRD pattern of 2GR EAFD sample

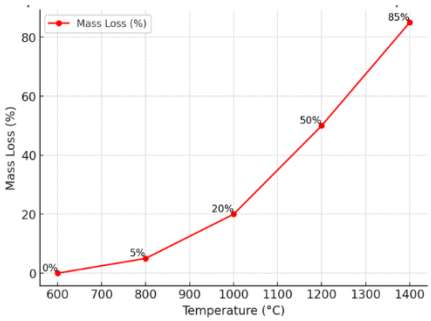

Figure 5. Dependence of zinc oxide mass loss on reduction temperature

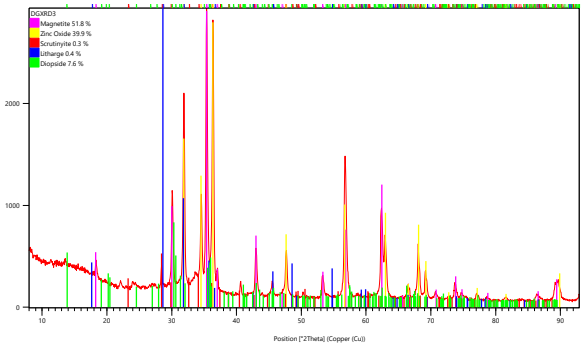

Figure 9. XRD pattern of 3RS EAFD sample

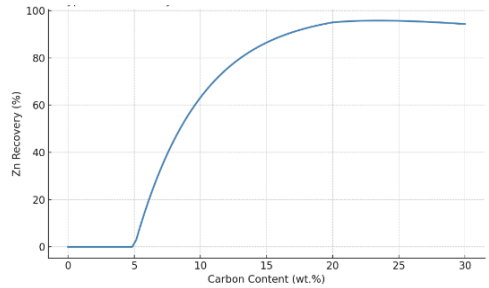

Figure 6. Zinc recovery vs carbon content in carbothermic reduction of zinc oxide

Zinc oxide is challenging to reduce. Its reduction temperature is 1100 °C. The presence of Franklinite, common in EAFD, indicates the occurrence of complex spinel phases. The reduction process of $ZnFe_2O_4$ involves three steps: $ZnFe_2O_4 \rightarrow FeO + ZnO \rightarrow Fe + ZnO \rightarrow Fe + Zn$ (g).

The thermodynamics of the reduction of synthetically prepared mixtures were studied. Mix 1 contains zinc oxide and carbon, Mix 2 contains Fe2O3-ZnO-C in an amount of carbon relative to the stoichiometrically calculated amount, and Mix 3 contains twice the amount of reducing agent. Mix 4 contains the EAFD presented in Table 1. From the experiments carried out by measuring EMF in a galvanic cell, equations of the dependences of the change in ΔGexp.= f(T) have been derived. The theoretical (Table 2) and experimental models are compared graphically in Figure 7.

ΔG° (J/mol)	R^2
Mix 1 ΔG° = 279802− 214·T	0.9671
Mix 2 ΔG° = 204654 - 164,79 T	0.9029
Mix 3 ΔG° = 119742-89,267·T	0.8786
Mix 4 ΔG° = 82636-81,78·T	0. 8482

The reaction ZnO+Fe=Zn+FeO is thermodynamically impossible in the studied temperature range.

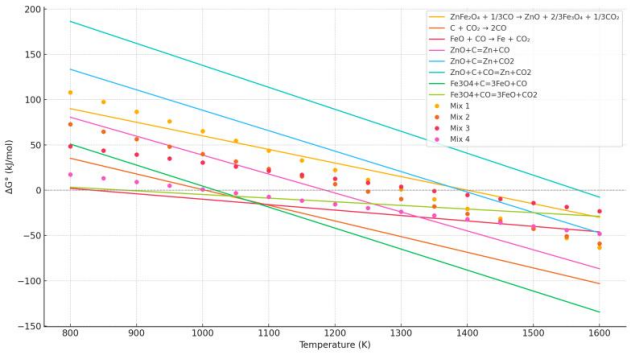

Figure 7. Gibbs Free Energy vs Temperature

Carbon usage below 5 wt.% is low and insufficient for reduction. A sharp increase in zinc recovery is observed with carbon contents of 5–20 wt.%. However, at higher carbon levels (>20 wt.%), zinc recovery either plateaus or declines, likely due to the onset of side reactions, reoxidation phenomena, or reduced process efficiency. Within the temperature range of 600–1000 °C and under carbon-rich conditions, zinc volatilizes into the gas phase, while iron oxides are reduced potentially to metallic iron accompanied by significant evolution of CO and CO_2. At elevated temperatures (>1200 °C) with an excess of carbon, iron may absorb carbon and form Fe–C alloys. Under such conditions, zinc losses may occur due to volatilization or carbide formation. In particular, reactions with excess carbon can lead to the formation of zinc carbide (ZnC_2) or promote the reverse oxidation of metallic zinc via the reaction: $Zn + CO \rightleftharpoons ZnO + C$. This reversible reaction may result in partial reoxidation of the reduced zinc back to ZnO.

4. CONCLUSION

The investigated samples, collected from three distinct regions, reflect variations in production technologies, raw material composition, and oxidation conditions. The identified predominant structural phases include magnetite, zinc oxide, and franklinite, as well as a crystallized calcium–magnesium silicate phase. The behavior of synthetic experimental mixtures aligns closely with theoretical predictions and provides insight into the underlying reduction mechanisms. Effective reduction is achieved when the carbon content in the charge is maintained between 15–20 wt.%. Excess carbon does not enhance reduction efficiency and may instead promote undesirable side reactions, zinc losses, increased fuel consumption, and elevated greenhouse gas emissions.

REFERENCES

[1] I. Ivanchev, Modern Steelmaking Processes. Theory and Practice, Sofia, 1994, p. 358.
[2] D. Llewellyn, R. C. Hudd, Steels metallurgy and applications, Elsevier Science, 1998.
[3] O. Ruiz, C. Clemente, M. Alonso, F.J. Alguacil, J. Hazard Mater., 141 (2007), 33-36.
[4] Tsv. Dimitrova, I. Zhabinski, et al., Industry and Environment, Sofia, 1993, p. 140.
[5] F. Kukurugya, T. Vindt, T. Havlík, Hydrometallurgy, 154 (2015), 20-32.
[6] E. Aries, G. Benavides et al., BAT for the ferrous metals processing industry, Office of the European Union, Luxembourg, 2022.
[7] J.M.A. Geldenhuis, Recovery of valuables from flue dust fines, Minerals Engineering, 2002.
[8] A.G. Guézennec et al., Powder Technol. 157(1-3), (2005), 2-11.
[9] D. Grigorova, R. Paunova, Metalurgija. 61(1) (2022), 189-92.
[10] J.M. McClelland, G.E. Metius, JOM, 55, (2003) 30–34.
[11] M.H. Morcali, O. Yucel et al., J. Min. Metall. Sec. B Metall., 48(2), (2012) 173-184.
[12] V.A. Shumskiy, et al. Russ. J. Non-Ferrous Met 60(3), (2019) 259–267.